

A STUDY OF THE TOKAMAK DE VARENNES PLASMA DURING FAST CURRENT RAMP-DOWN: EXPERIMENT AND SIMULATION RESULTS WITH THE TSC CODE

M.M. SHOUCRI, I.P. SHKAROFSKY, G.W. PACHER*, H.D. PACHER*,
J. KALNAVARNS, P. COUTURE, R. DECOSTE, B.C. GREGORY,
E. HADDAD, C. JANICKI, J.-L. LACHAMBRE, G. LeCLAIR, N. RICHARD,
C. SIMM, M. St. ONGE, D. WHYTE and Tokamak de Varennes Team
Centre canadien de fusion magnétique,
Varennes, Québec,
Canada

N. POMPHREY, S.C. JARDIN
Princeton Plasma Physics Laboratory,
Princeton University,
Princeton, New Jersey,
United States of America

ABSTRACT. Simulation results obtained with the axisymmetric Princeton Tokamak Simulation Code TSC are compared with experimental results for the time evolution of the Tokamak de Varennes plasma. The code correctly predicts experimental conditions; of special interest are the favourable comparisons of the simulation with experiments during fast current ramp-down (from 250 kA in 40 ms, three times faster than the L/R time).

1. INTRODUCTION

This paper presents experimental results for the evolution of the Tokamak de Varennes (TdeV) plasma during fast current ramp-down, and compares these results with the predictions of the Princeton Tokamak Simulation Code (TSC) [1]. This code was developed to model the axisymmetric evolution of a toroidal plasma due to plasma transport and resistive dissipation, and the positional stability and control properties of a tokamak. The plasma interacts with a discrete set of axisymmetric conductors which model the poloidal field coil system and the vacuum vessel. The coils obey realistic circuit equations which model the feedback systems used in the experiment. The plasma remains in force balance equilibrium, consistent with the fields of the poloidal field coil currents and of the induced currents in the vacuum vessel, while the plasma's own current and pressure distribution evolves owing to transport processes. A two-fluid model is used, with separate ion and electron

temperatures. The vacuum is treated as the limit of a very high resistivity, zero pressure plasma. The code is described in detail in Ref. [1].

Motivation for studies of fast ramp-down and ramp-up originates in plans to operate the TdeV in the quasi-continuous mode. This means increasing the cumulative time of successive Ohmic discharges up to the maximum duration of the toroidal magnetic field (eventually, 30 s). The interval between successive discharges is limited mainly by the time required for the vacuum gas conditions to reach a suitable state for initiation of the next discharge pulse. Obviously, a rapid and smoothly controlled ramp-down discharge pulse would return a significant part of the stored magnetic energy to the electrical power source and could in this way minimize the impurity evolution from the inner walls of the vacuum vessel. Fast ramp-down of the plasma current from its plateau value to zero, in a controlled manner, avoiding disruptions, might be important for all tokamaks, but particularly for large ones such as TFTR, JET, JT-60 and T-15, and future machines such as ITER and CIT. This is because the large amount of kinetic and magnetic energy stored in the device could easily damage limiter plates, vacuum

* Present address: NET Team, Max-Planck-Institut für Plasmaphysik, Garching bei München, Germany.

vessel, divertor plates, etc., if it were unleashed in an uncontrolled way. Moreover, these large machines have very long resistive time constants (L/R of several seconds), and it may be desirable to bring the discharge to a controlled termination and to remove the stored energy in times shorter than these. Also, the lengthening of the plasma current plateau by fast current ramp-up is especially relevant to copper coil machines. Finally, from the operation point of view, a better understanding of large and fast current transients is desirable, since it is well known that the fast current variations have significant influence on MHD activity and current shaping.

For the experiments described here, the TdeV was operated using only Ohmic heating in single-pulse operation. The plasma is limited by a set of four poloidal graphite limiters, and the walls are of stainless steel. At present, the minor radius is 0.24 m, the nominal major radius is about 0.86 m and the toroidal field is 1.5 T. The plasma current plateau is normally 200 kA ($q \sim 3.0$), but operation up to 295 kA ($q \sim 2.0$) has been achieved. The line averaged densities are typically $(2-4) \times 10^{19} \text{ m}^{-3}$, measured with a six-channel 0.214 mm interferometer.

For currents between 180 and 250 kA, the TdeV plasma is characterized by a central electron temperature of 700–800 eV, measured by Thomson scattering. The temperature profiles are obtained from soft X-ray pulse height analysis. The ion temperature profile is measured by the Doppler broadening of impurity lines (O VII, C IV and Ne IX) and is found to be about 500 eV at the centre.

The global energy confinement time is found to be 8.5 ms, which is in good agreement with the value of 8.6 ms obtained from the neo-Alcator scaling of Ohmic plasmas [2]. The value of Z_{eff} , deduced from a multi-channel measurement of the bremsstrahlung continuum in the visible range, is found to be about 3–4 in the centre; it is relatively flat as a function of minor radius and increases slightly when the hydrogen plasma is contaminated with 0.5% Ne. Further details on the TdeV plasma parameters have been presented recently [3].

The ability of the TSC code to reproduce experimental shot data was demonstrated previously [4]. The present paper further validates the code against experimental data from the TdeV, in particular by a comparison with a fast current ramp-down experiment in which the plasma current is forced to zero in a controlled way. Experimental plasma current ramp-down limits are being explored using the external equilibrium field coils driven by preprogrammed wave forms. However,

the TdeV will be equipped in the near future with a fast position control system using coils inside the vacuum vessel to improve the control of the plasma during forced ramp-down of the plasma current.

Section 2 describes details of the TdeV that are incorporated in the TSC code. Section 3 discusses the results for a forced fast ramp-down of the plasma current, and Section 4 presents the conclusions.

2. THE TSC CODE MODEL FOR THE TdeV

The toroidal vacuum vessel is a rigid torus of rectangular cross-section, made of type 316L stainless steel. It is constructed in two halves, with two electrical breaks in the vertical plane, and with 16 bays at the top, the bottom and the outside of the vessel. The TSC code models the vacuum vessel as a series of axisymmetric wire filaments (92 wires), with resistance and inductance calculated to match those of the true vessel structure. The vacuum vessel time constant for the penetration of the vertical field is approximately 5 ms [5]. Plasma control on the TdeV is carried out by real-time feedback loops on the radial plasma position, the vertical position, the plasma current and the density. The TSC code uses feedback systems to control these variables, with the exception of the density, which is preprogrammed to follow the experimental value.

The control wave forms of the TdeV [6] are produced digitally, using a programmable high speed controller (PHSC). The plasma position is monitored by magnetic flux and magnetic field measurements, which are used to extrapolate the measured fluxes to the desired location of the plasma surface. The plasma major radius R_0 is calculated using combinations of signals from flux loops, saddle coils, and coils wound in a 'figure eight' configuration which give the effective fluxes and their first and second spatial derivatives at points on the midplane outside and inside the plasma. The desired value of R_0 is defined by two points representing the intersections of the nominal outer flux surface of the plasma with the midplane. The control signal for the plasma position is the flux difference corresponding to the two points; this signal enters a proportional integral controller in the control algorithms. The model in the TSC code is similar.

In addition to the feedback loop on the plasma major radius, there is an additional PI feedback circuit within the vertical field EF power supply itself, with a separate PHSC system which drives the output current to follow the input wave form. Thus, from a theoretical point of

view, the control of the vertical field is a two-level process, with an external feedback loop generating the desired current and an internal feedback loop representing the power supply action to follow the reference signal. A similar system is used in the TSC code, where the desired currents are the sum of a preprogrammed part and a PI feedback signal. An internal feedback loop within TSC controls the voltages of the coils to force the currents to follow the desired preprogrammed values. The OH power supply is operated by voltage control using a feedback signal calculated with a PI block which acts on the difference between the measured and the required plasma currents. Simulation of a complete shot for the TdV gives good agreement with experimental results.

3. FORCED CURRENT RAMP-DOWN

Forced current ramp-down has been studied using a preprogrammed vertical field during the ramp-down phase generated by coils external to the vacuum vessel, with a penetration time of about 5 ms [5]. The present calculation simulates shot 5027, in which the plasma current is brought down to 40 kA from an equilibrium value of 250 kA at a rate of 6 MA/s, approximately three times faster than the L/R decay rate. Because of

the rapid time-scale involved, the feedback circuit on the vertical field is not effective. While the plasma current was successfully ramped down to zero without disruption in this shot, insufficient adjustment of the preprogrammed vertical field in the experiment caused the plasma to hit the outer limiter when the plasma current was about 40 kA. The equilibrium plasma had $Z_{\text{eff}} \sim 4$ (hydrogen plasma with 0.5% Ne), and a peak electron temperature of about 800 eV and an ion temperature of 500 eV for a peak density of $3.6 \times 10^{19} \text{ m}^{-3}$. Figure 1 shows a section representation of the equilibrium of the TdV at 250 kA calculated by the TSC code.

A simple sawtooth model has been combined with the previously reported Coppi-Tang thermal diffusivity model [4] to more accurately reproduce the experimentally observed flattening of the temperature profile in the central region. The model consists of enhancing the thermal conductivity by a factor of ten inside the $q = 1$ surface and applying an overall factor of 0.7. These two factors affect only the profile shape and result in the same global energy confinement time compared to the model with no sawtooth region. The temperature profile calculated from the transport obtained with the TSC code gives a peak electron temperature close to 800 eV and a peak ion temperature close to 550 eV at equilibrium. The electron density profile is obtained

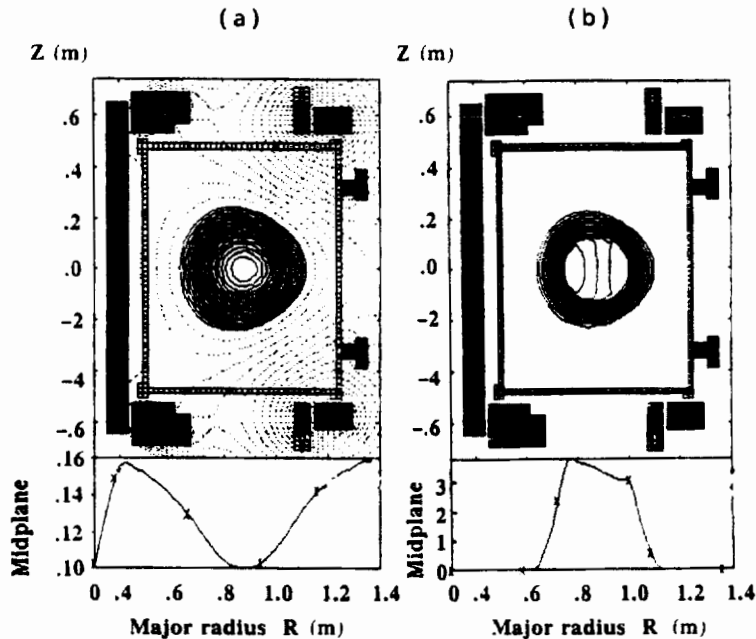


FIG. 1. Equilibrium plot of (a) the poloidal flux and (b) the current density profile, for a total plasma current of 250 kA.

from the multichannel 0.214 mm interferometer data which are Abel inverted, assuming density contours coincident with the flux surfaces as calculated from the equilibrium code. In the TSC simulation, the density profile was chosen to evolve in time according to

$$n(\psi, t) = n(t) \left[1 - \left(\frac{\psi - \psi_{\min}}{\psi_{\text{lim}} - \psi_{\min}} \right)^2 \right]^{0.5}$$

where the peak density has been adjusted to fit the experimental values. The equilibrium has a volume averaged beta of 0.41% and a poloidal beta of 0.18.

The current was ramped down from an initial value of 250 kA at an initial time $t_i = 650$ ms to a final value of 40 kA at $t = 688$ ms. The ramp-down simulation with the TSC code was effected by programming the measured experimental values for the plasma current, the position of the plasma centre and the current variation in the Ohmic and vertical field coils. In addition, a small proportional feedback was applied to the vertical field coils to enforce the plasma centre position that had been preprogrammed. However, no feedback was applied to the Ohmic current variation which controls the plasma current in the simulation;

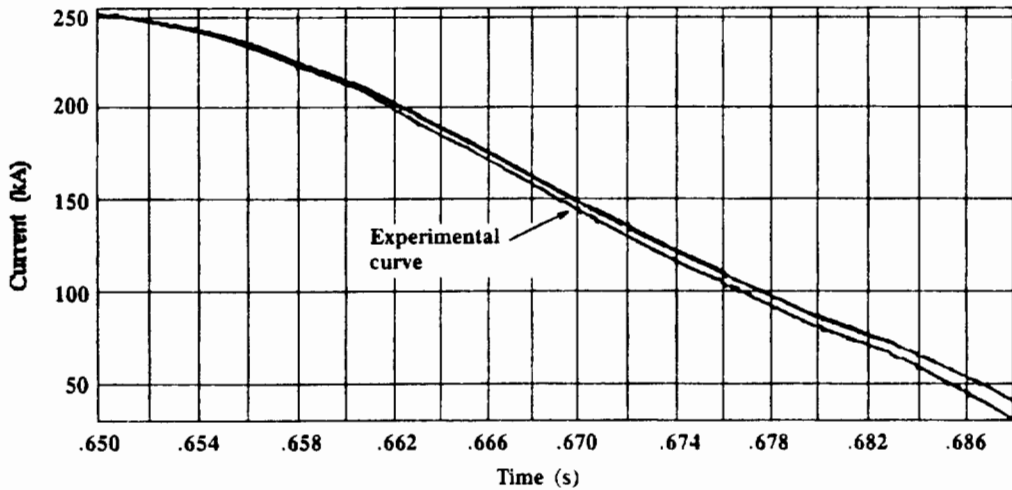


FIG. 2. Time evolution of the total plasma current during current ramp-down calculated by the TSC code, together with the experimental value.

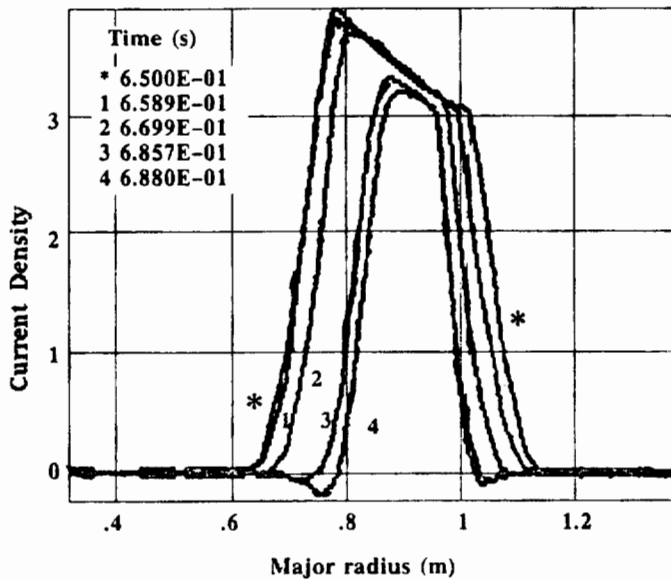


FIG. 3. Time evolution of the current density profiles during ramp-down calculated by the TSC code. Note the appearance of the negative skin layer current.

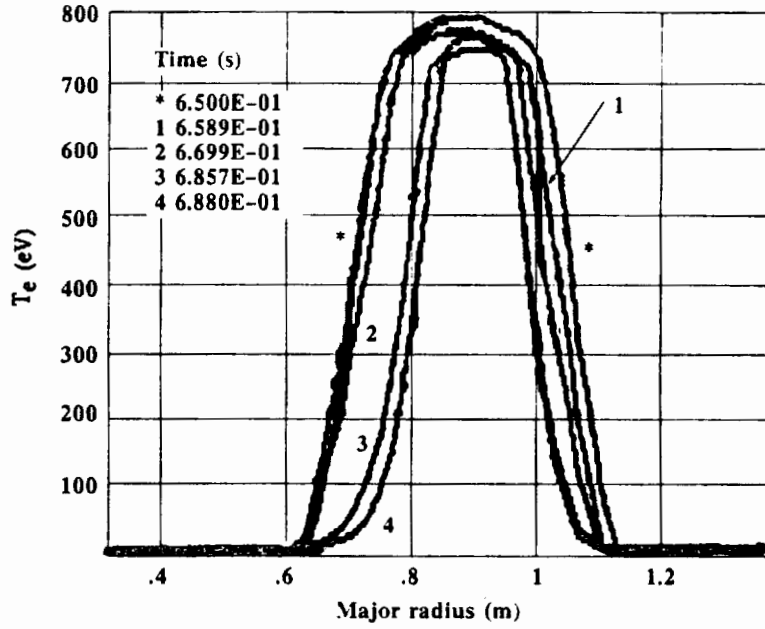


FIG. 4. Time evolution of the electron temperature profile during current ramp-down (from $t = 650$ ms to $t = 688$ ms).

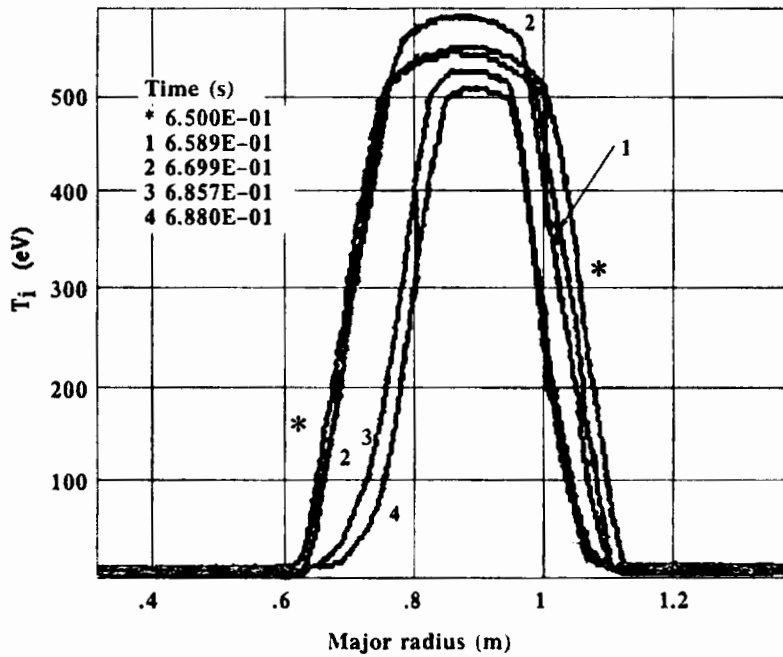


FIG. 5. Time evolution of the ion temperature profile during current ramp-down (from $t = 650$ ms to $t = 688$ ms).

the TSC code was nonetheless able to reproduce almost exactly the experimentally observed and pre-programmed plasma current variation.

Figure 2 shows the time evolution of the experimentally measured total current during the ramp-down, together with the current calculated by the TSC code. The agreement between the experimental values and the simulation values for the current in the coils is also very good. Figure 3 shows the time evolution of the current density profiles during ramp-down, calculated by the TSC code; it clearly shows the formation of a small negative skin current for this rapid ramp-down. A similar result was also obtained in previous simulations [8, 9]. Figure 3 also shows that the peak central value decreases only slowly; this trend is in qualitative agreement with the evolution of the soft X-ray profiles. Figures 4 and 5 give the time evolution of the temperature profiles for the electrons and ions during ramp-down. The peak temperatures have a tendency to remain approximately constant. Similar results have been observed experimentally during fast ramp-down of the plasma current on ASDEX [10].

Figure 6 shows the experimentally observed electron density profiles during current ramp-down in time steps of 5 ms. The density evolution during this phase is characterized by a progressive change of the profile from a flat shape at 250 kA to a peaked shape at 70 kA, with a respective decrease in the peak density.

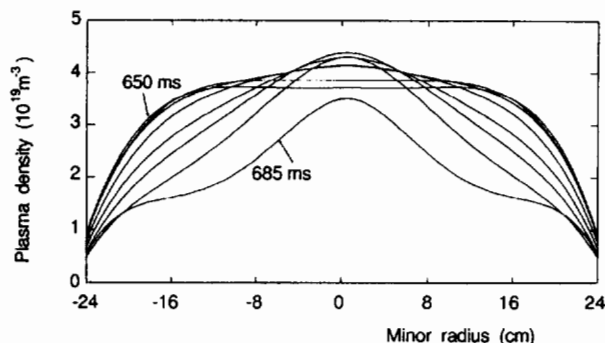


FIG. 6. Electron density profiles during the forced current ramp-down from 250 kA to 70 kA, at a rate of 6 MA/s, as observed with the submillimetre wave interferometer. The time step between profiles is 5 ms.

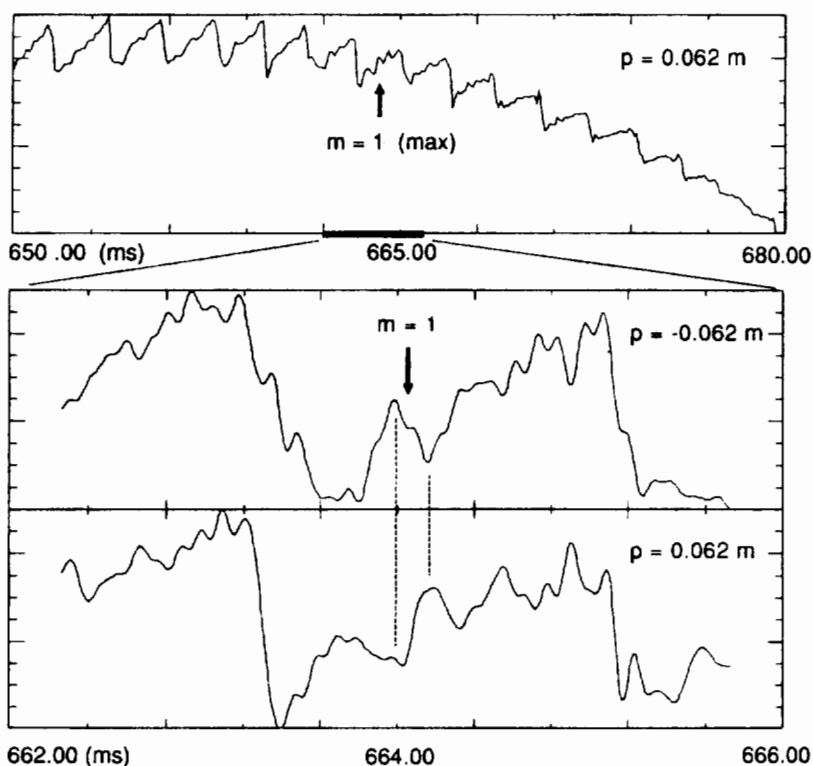


FIG. 7. Time evolution of the sawtooth oscillations observed close to the $q = 1$ surface at ± 6.2 cm, showing that the $m = 1$ kink oscillation increases around $t = 665$ ms, when the $q = 3$ surface penetrates the edge of the plasma.

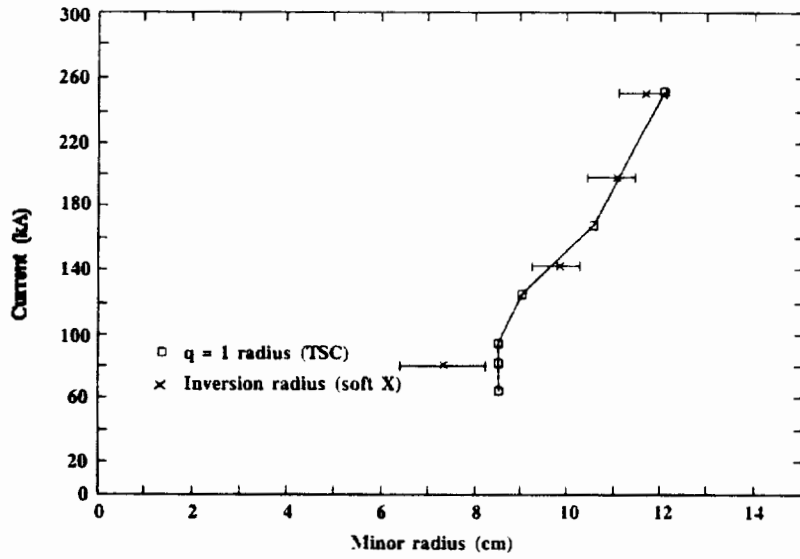


FIG. 8. Comparison of the sawtooth inversion radius obtained from soft X-ray measurements with the radius of the $q = 1$ surface deduced from the TSC code.

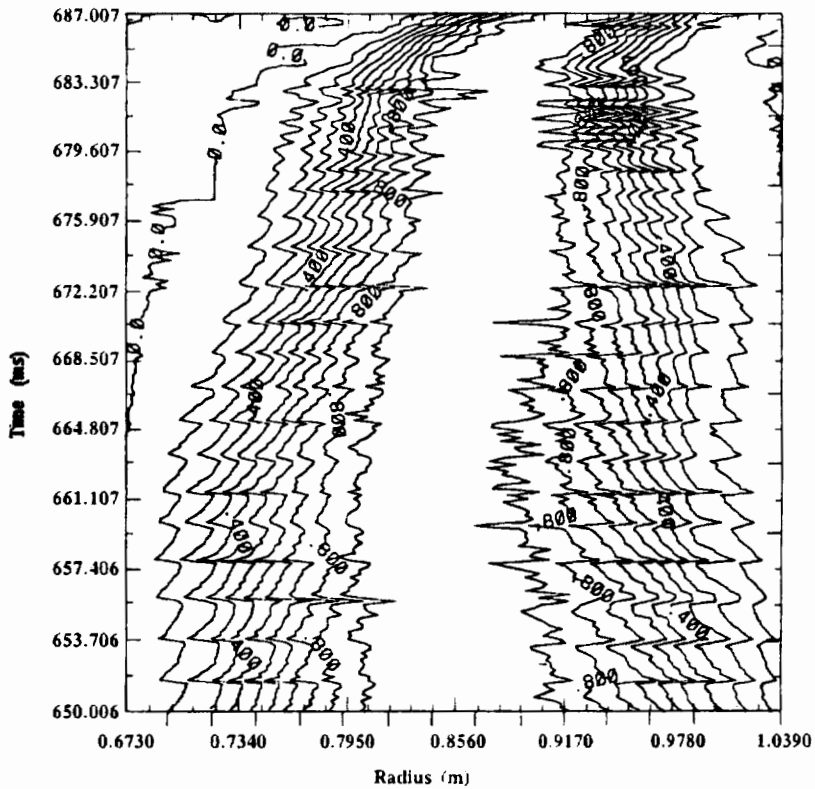


FIG. 9. Time evolution of the contour plots of the soft X-rays between 650 ms and 687 ms as seen from the upper vertical camera.

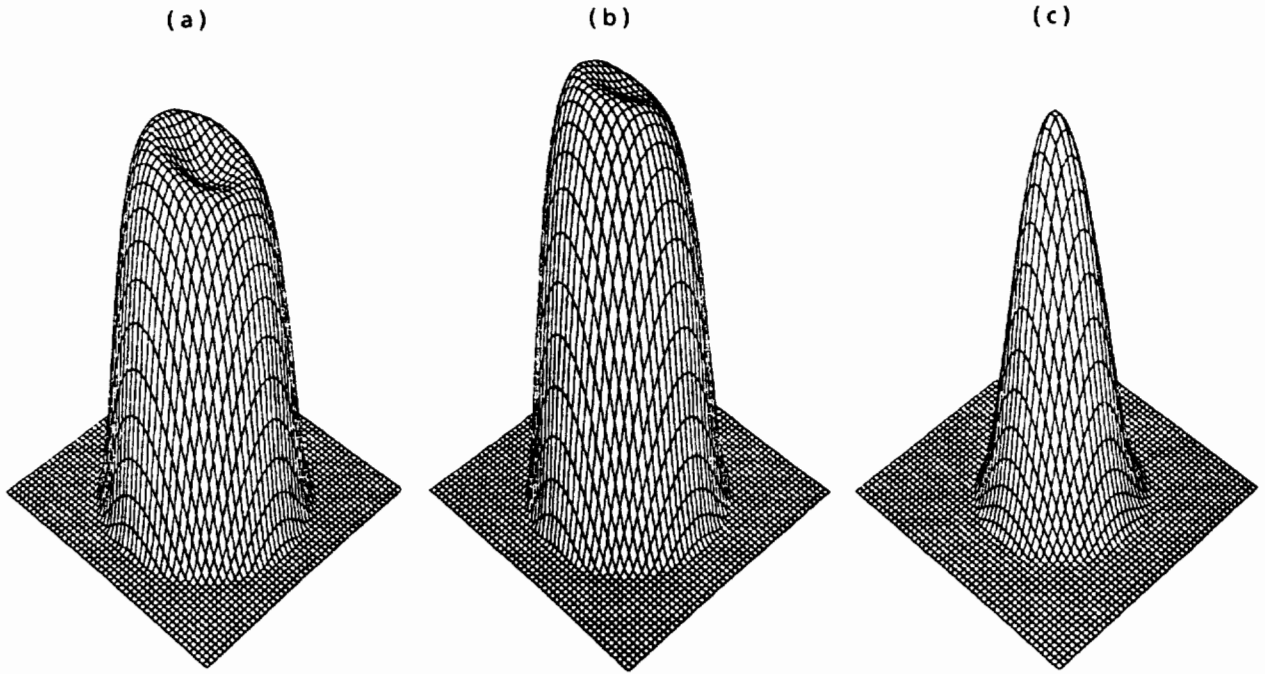


FIG. 10. Three-dimensional plot of the soft X-ray signals during ramp-down of the plasma current at (a) 650 ms, (b) 665 ms and (c) 680 ms. The decrease in the thickness of the profile can be clearly seen.

Soft X-ray measurements have indicated the variation of the $m = 1$, $n = 1$ internal kink mode during ramp-down (Fig. 7). The results obtained using PEST2 [11] show that the eigenvalue of the linearly unstable ideal MHD kink mode reaches a peak at $t \sim 665$ ms, at the time when the plasma current is ~ 216 kA and the $q = 3$ surface is just inside the plasma radius. This is in agreement with experimental observation. Figure 7 illustrates the measured soft X-ray signal at 6.2 cm from the centre, close to the $q = 1$ surface, showing an increase of the amplitude of the $m = 1$ oscillation superimposed on the sawteeth at around 665 ms and also an amplification of the oscillations at around $t = 665$ ms on opposite sides of the centre, clearly identifying the $m = 1$ oscillations.

In Fig. 8, the sawtooth inversion radius obtained from soft X-ray measurements is compared with the radius of the $q = 1$ surface deduced from the TSC code during ramp-down; the radii agree within the experimental error. However, the experimental uncertainty in the inversion radius at low current (below 100 kA) is so large that the constant position of the $q = 1$ surface, seen in Fig. 8, does not constitute a definite proof of the inverted current density layer as indicated by the TSC code (Fig. 3). Figure 9 shows

the time evolution of the contour plots of the soft X-rays between 650 ms and 687 ms as observed with the upper vertical camera. It can be seen that there is a decrease in the width of the profile and a small displacement outward, similar to that calculated by the TSC code for the current density profile (Fig. 3) and for the temperature profiles (Figs 4 and 5). Figure 10 is a three-dimensional plot of the soft X-ray signals and shows clearly the decrease in thickness of the profile during the ramp-down of the plasma current, while the peak is varying slowly.

Figure 11 shows the time evolution of the plasma surface loop voltage during the current ramp-down. Figure 12 shows the time evolution of the parameter $\beta_p + \ell/2$. Both parameters follow closely the values calculated by the TSC code. The simulation curve was computed from the definition

$$\beta_p = 4 \int \rho dV / \mu_0 R_0 I_p^2$$

$$\ell = \int B_p^2 dV / \mu_0^2 R_0 I_p^2$$

where the integrals are over the entire plasma volume. The agreement between the experimental value and the simulation is good. To give some pattern to the study

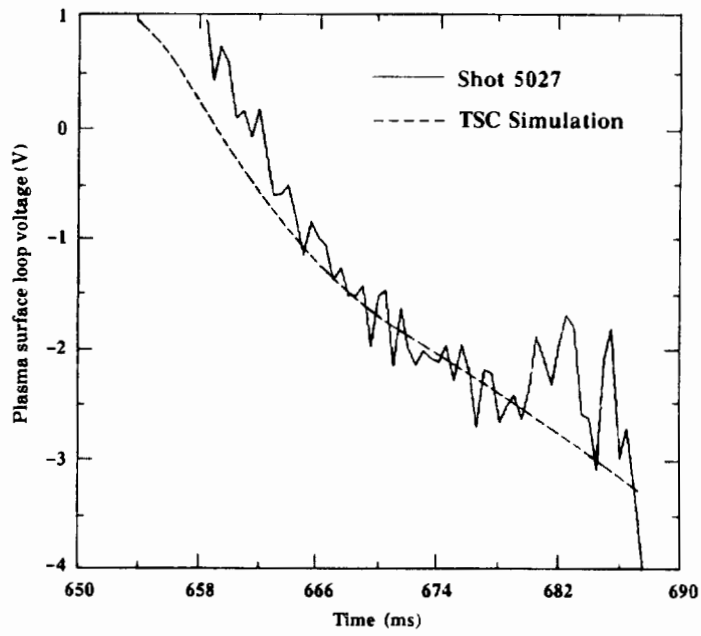


FIG. 11. Time evolution of the plasma surface loop voltage during ramp-down of the plasma current.

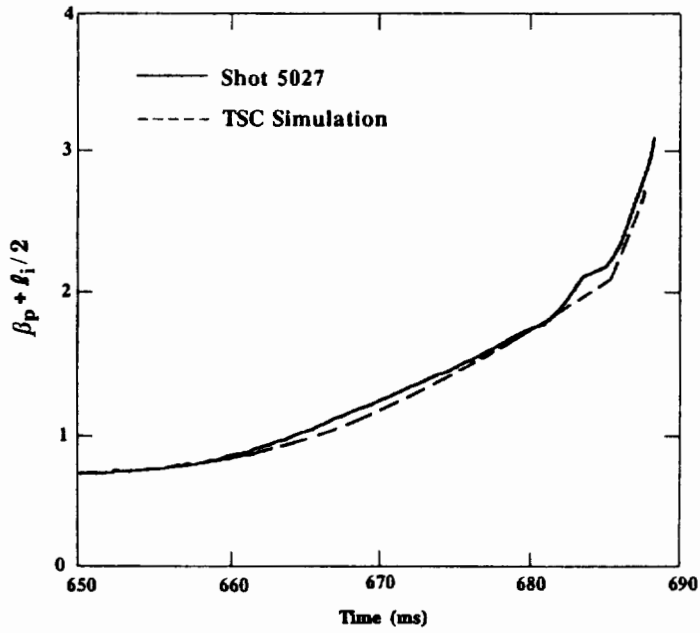


FIG. 12. Time evolution of the parameter $\beta_p + l_i/2$ during ramp-down of the plasma current.

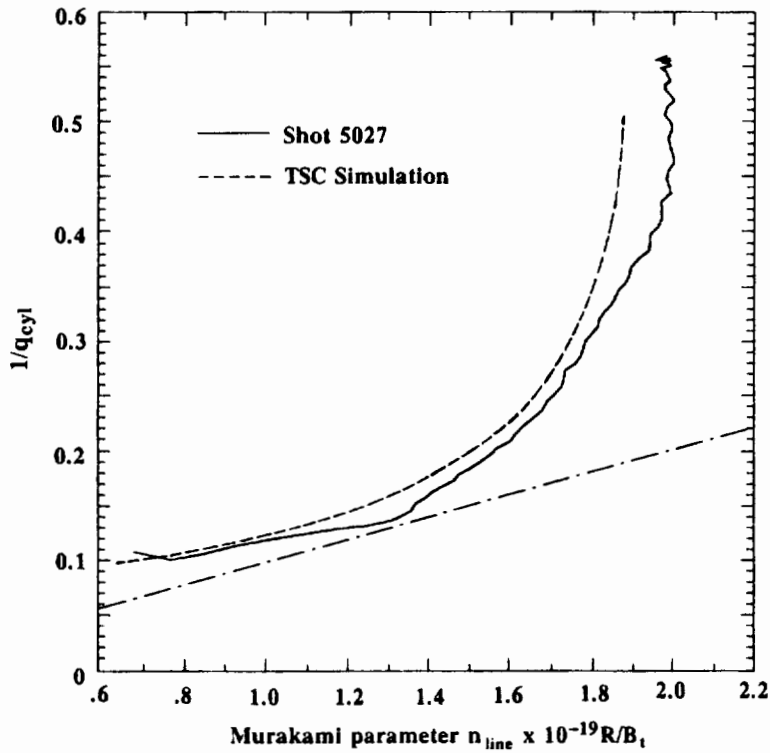


FIG. 13. Representation of the ramp-down process on the Hugill diagram. The straight line indicates the Hugill limit of 10.

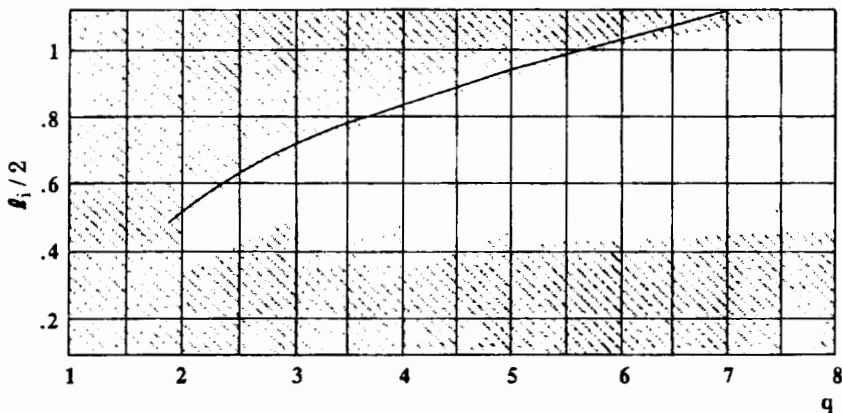


FIG. 14. Trajectory of the discharge on the $l_i/2 - q_{edge}$ plane.

of disruptions, it is common to use the Hugill diagram. Figure 13 gives a representation of the ramp-down process on the Hugill diagram. The initial conditions for the ramp-down, with a cylindrical q value of less than 2, correspond to an equilibrium q value of approximately 2. As the ramp-down proceeds, the parameters approach the dashed line representing the Hugill limit

of 10. However, as pointed out in Refs [12] and [13], the operational aspects can be seen from another point of view, using a different diagram with the parameters q_{edge} and the internal inductance $l_i/2$. Figure 14 shows the trajectory during ramp-down in this operational space, located close to the density limit, as defined in Refs [12, 13].

4. CONCLUSIONS

Good agreement is found in a comparison of the results obtained with the tokamak simulation code TSC, using an empirical thermal conductivity model and neoclassical resistivity, with experiments on TdeV discharges during fast current ramp-down. Successful simulation has been achieved of disruption-free current ramp-down from 250 kA at a rate of 6 MA/s, three times faster than the L/R rate, using a preprogrammed vertical field. Of special interest during the simulation of the ramp-down is the fact that the peak value of the current profile decreases very slowly, while the profile is narrowing at the periphery. The linear stability of the $m = 1$, $n = 1$ mode has been investigated during ramp-down using the PEST2 code; there is a maximum amplitude when $q(a) = 3$ on the plasma surface, in qualitative agreement with the experiment. The TSC code appears to be a useful tool for the study of the faster ramp-down rates obtainable with the fast horizontal position feedback coils being installed inside the vacuum chamber of the TdeV. These additional coils will permit effective feedback control during ramp-down and studies on the limit of the ramp-down rate.

ACKNOWLEDGEMENTS

The authors are grateful to Dr. A. Boileau for reading the manuscript and for useful comments, and to Dr. J. Manickam for assistance with the PEST2 stability code. This work was supported by the Centre canadien de fusion magnétique and MPB Technologies. The Centre canadien de fusion magnétique is a joint venture of Hydro-Québec, the Atomic Energy of Canada Ltd (AECL) and the Institut national de la recherche

scientifique (INRS), in which MPB Technologies Inc., Canatom Inc. and the Université de Montréal also participate. It is principally funded by AECL, Hydro-Québec and INRS.

REFERENCES

- [1] JARDIN, S.C., POMPHREY, N., De LUCIA, J.L., *J. Comput. Phys.* **66** (1986) 481.
- [2] GOLDSTON, R.J., *Plasma Phys. Controll. Fusion* **26** (1984) 87.
- [3] BOLTON, R.A., ABEL, G., BÉLANGER, C., et al., in *Plasma Physics and Controlled Nuclear Fusion Research 1988 (Proc. 12th Int. Conf. Nice, 1988)*, Vol. 1, IAEA Vienna (1989) 495.
- [4] JARDIN, S.C., De LUCIA, J.L., OKABAYASHI, M., et al., *Nucl. Fusion* **27** (1987) 569.
- [5] KALNAVARNS, J., PACHER, G.W., PACHER, H.D., in *Fusion Engineering (Proc. 11th Symp. Austin, TX, 1985)*, IEEE, New York (1985) 469.
- [6] KALNAVARNS, J., DEMERS, Y., St. ONGE M., et al., in *Fusion Engineering (Proc. 12th Symp. Monterey, CA, 1987)*, IEEE, New York (1987) 1370.
- [7] JANICKI, C., DECOSTE, R., SIMM, C., *Phys. Rev. Lett.* **62** (1989) 3038.
- [8] PACHER, H.D., GREGORY, B.C., PACHER, G.W., *Nucl. Fusion* **26** (1986) 507.
- [9] SHKAROFSKY, I.P., SHOUCRI, M., *J. Plasma Phys.* **26** (1981) 481.
- [10] MURMANN, H., ZOHRM, H., and the NI Team, in *Controlled Fusion and Plasma Heating (Proc. 17th Eur. Conf. Amsterdam, 1990)*, Vol. 14B, Part I, European Physical Society (1990) 54.
- [11] GRIMM, R.C., DEWAR, R.L., MANICKAM, J., *J. Comput. Phys.* **49** (1982) 94.
- [12] CHENG, C.Z., FURTH, H.P., BOOZER, A.H., *Plasma Phys. Controll. Fusion* **29** (1987) 351.
- [13] WESSON, J.A., GILL, R.D., HUGON, M., et al., *Nuclear Fusion* **29** (1989) 641.

(Manuscript received 1 March 1990)

Final manuscript received 20 June 1990)